-Supplementary information-

Construction of organic inorganic hybrid composite derived from C_3N_5 incorporated with CeO_2 nanoparticles for the enhanced photocatalytic hydrogen evolution

Ashil Augustin[a], Manova Santhosh Yesupatham[a], M.D. Dhileepan[a], Sanguk Son[b], Ezhakudiyan Ravindran[a], Bernaurdshaw Neppolian[a], Hyoungil Kim[b*], and Karthikeyan Sekar[a*]

[a]*Department of Chemistry, Faculty of Engineering and Technology, SRM Institute of Science and Technology, Kattankulathur, 603203, India*

[b]*Department of Civil & Environmental Engineering, Yonsei University, Seoul 03722, Republic of Korea*

Corresponding Author E-mail: karthiks13@srmist.edu.in; hi.kim@yonsei.ac.kr

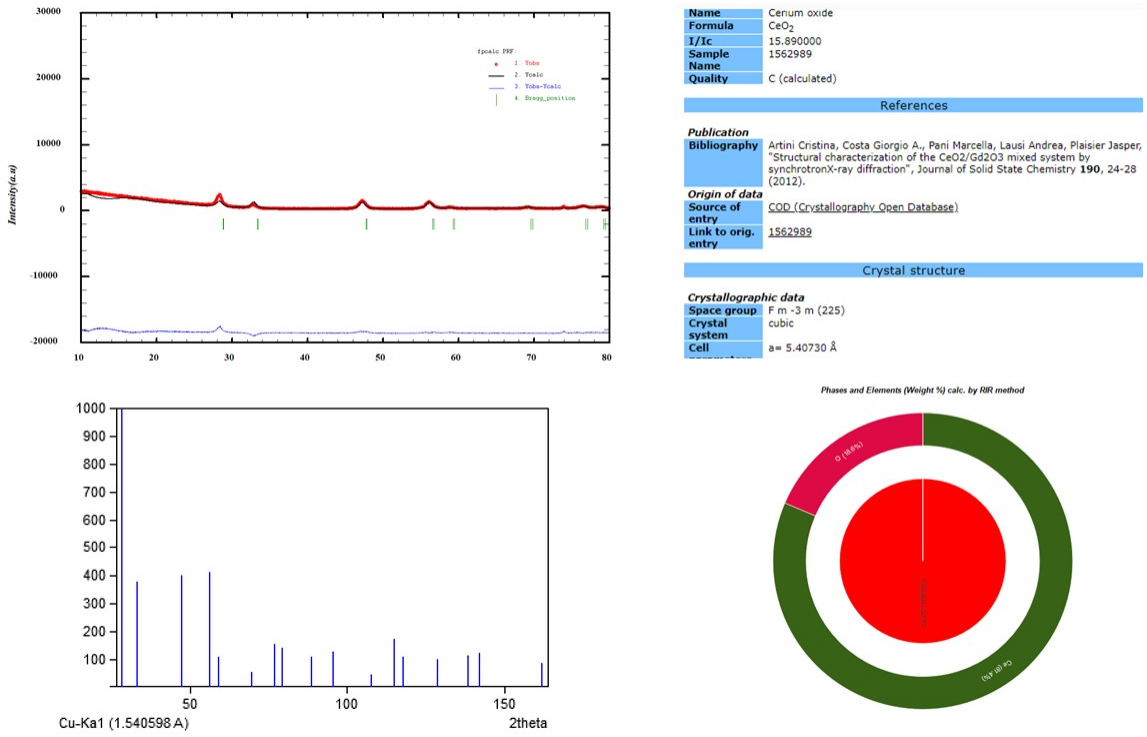

Figure S1. Rietveld analysis of CeO_2 photocatalyst and composition of the CeO_2 photocatalyst

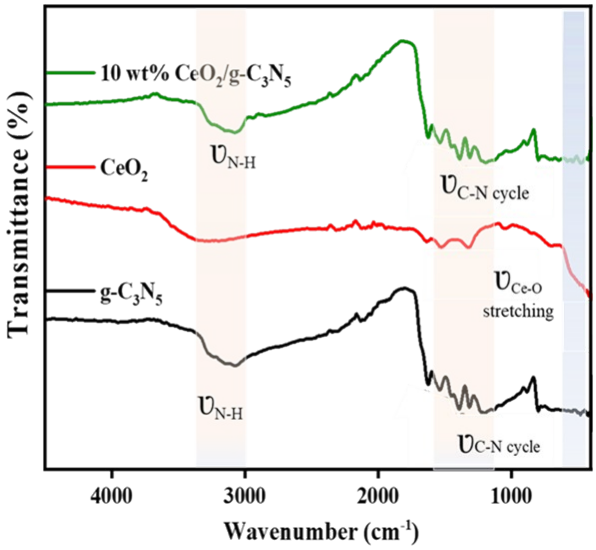

Figure S2. FTIR spectra of C_3N_5, CeO_2 and C_3N_5/CeO_2 Composite.

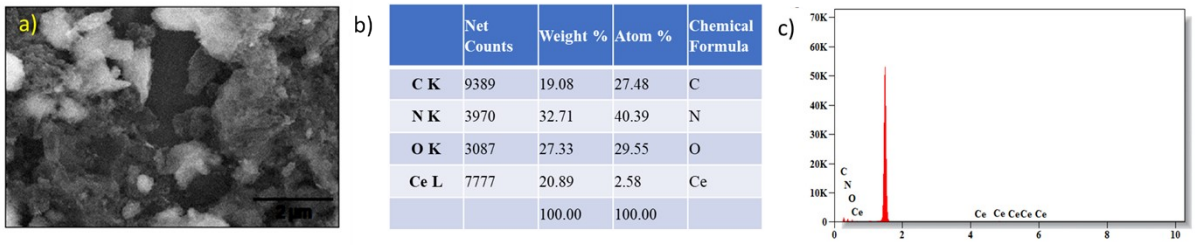

	Net Counts	Weight %	Atom %	Chemical Formula
C K	9389	19.08	27.48	C
N K	3970	32.71	40.39	N
O K	3087	27.33	29.55	O
Ce L	7777	20.89	2.58	Ce
		100.00	100.00	

Figure S3. a) SEM image (b-c) respective energy-dispersive spectroscopy ratio of the CeO_2/C_3N_5 composite (Ce, O, C, and N elements)

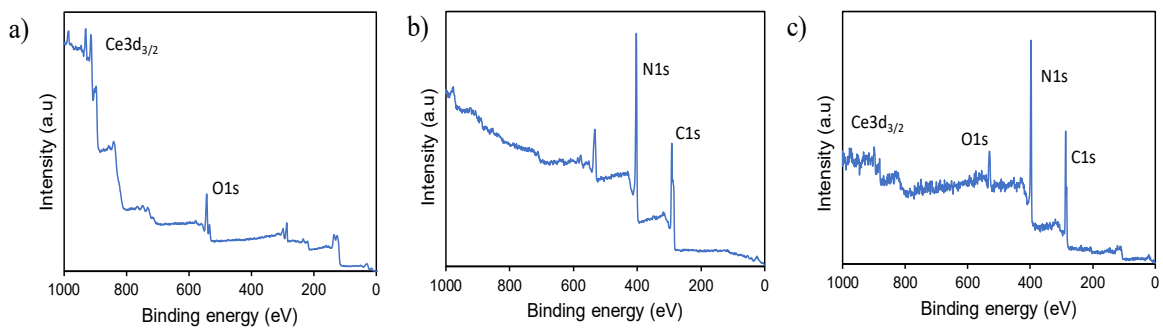

Figure S4. Survey XPS spectra of CeO_2, C_3N_5 and C_3N_5/CeO_2 Composite.

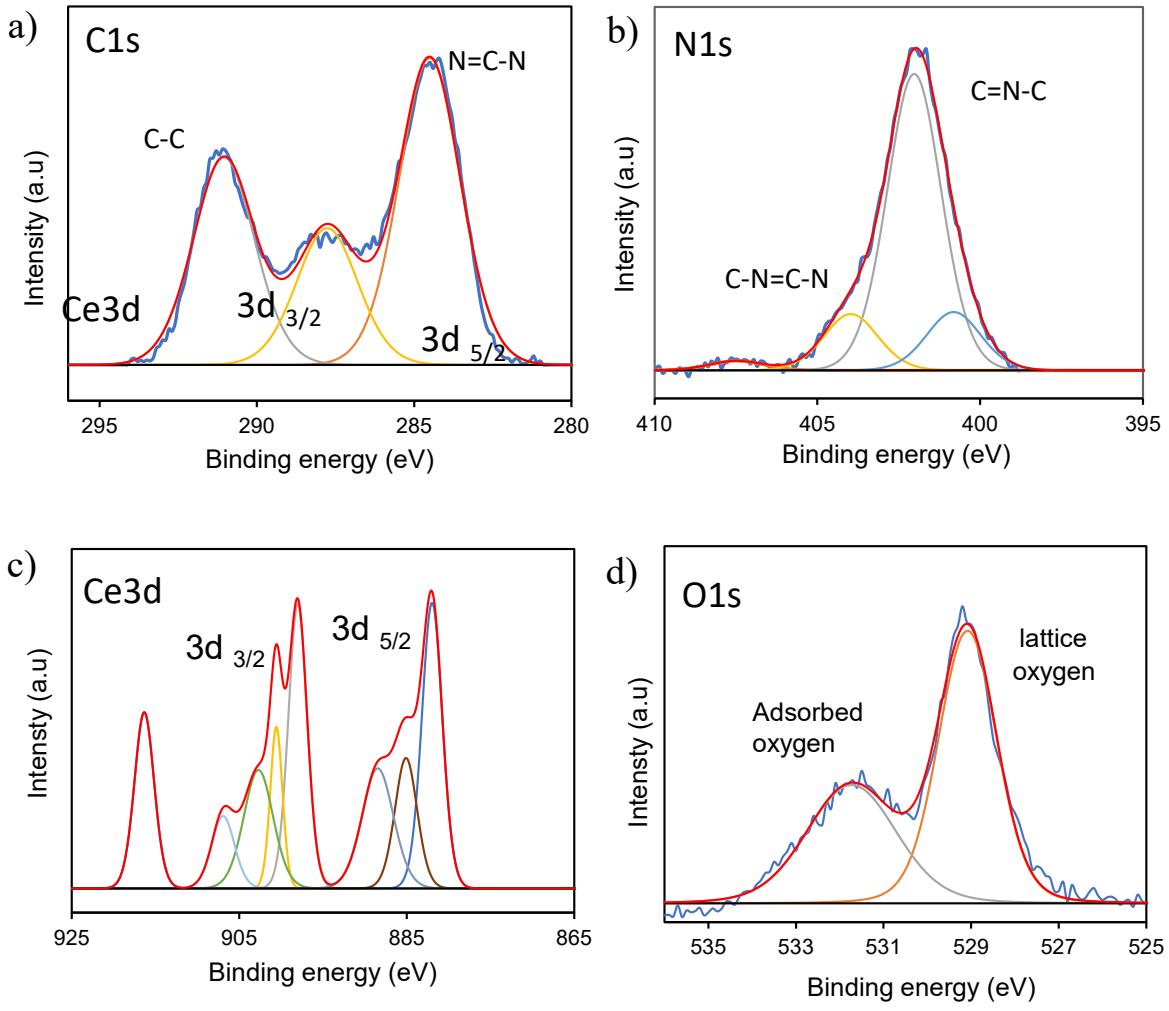

Figure S5. high resolution XPS of (a) C1s, (b) N 1s, (c) Ce 3d, (d) O 1s spectra of CeO_2 and C_3N_5 pristine materials.

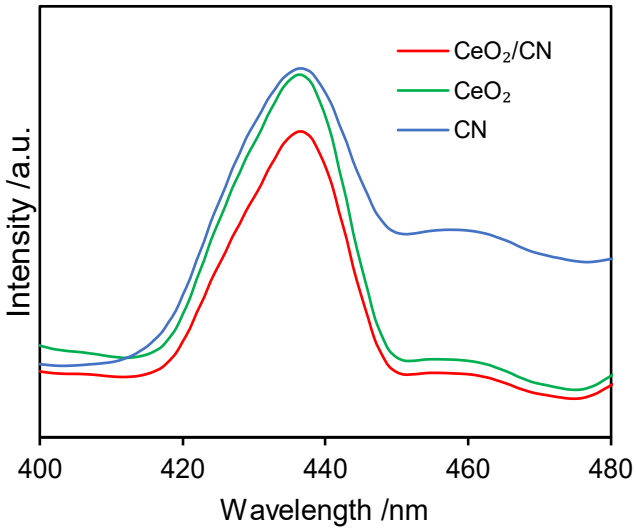

Figure S6. photoluminescence spectra of the samples.

The conduction band (CB) can be evaluated and converted to reversible hydrogen electrode (RHE) scale according to Nernst equation given as equation S1.

$$E_{RHE} = E_{Ag/AgCl} + E^{0}_{Ag/AgCl} + (0.059*pH) \quad (S1)$$

where E_{RHE} is the converted potential vs. RHE, $E^{0}_{Ag/AgCl}$ is 0.197 V, $E_{Ag/AgCl}$ is the experimentally measured potential against Ag/AgCl reference and pH of Na_2SO_4 electrolyte is 7 at 25 ℃. Further, the valence band (VB) was calculated using Equation S2:

$$E_{VB} = E_g + E_{CB} \quad (S2)$$

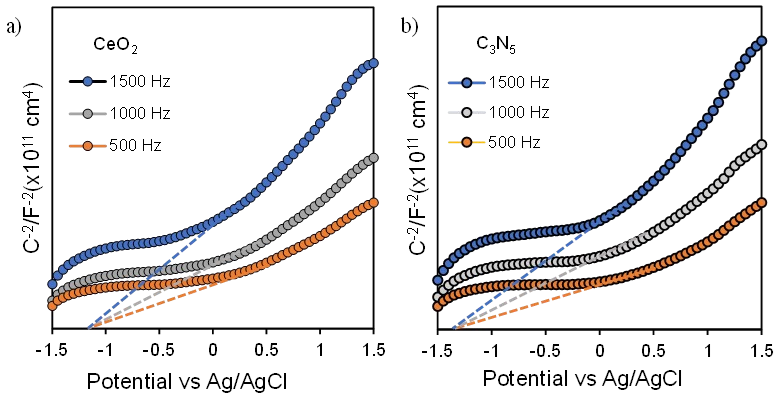

Figure S7. Mott–Schottky analysis of the samples a) CeO_2 b) C_3N_5

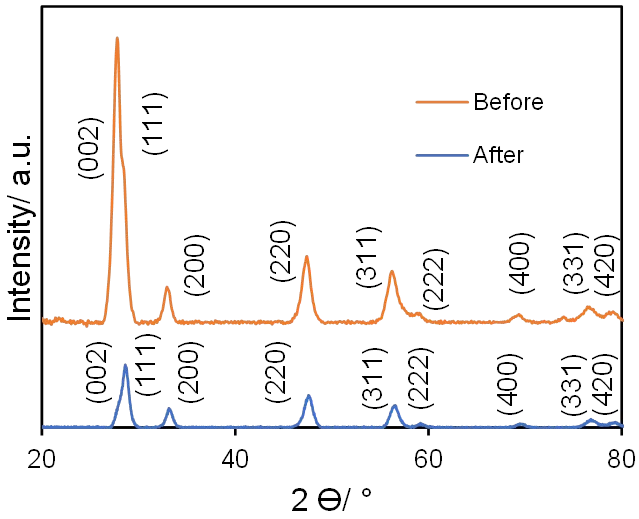

Figure S8. XRD analysis of C_3N_5/CeO_2 composite after and before the reaction study.

Table S1. Physiochemical properties of the pristine catalyst used for photocatalytic application

Catalyst	Crystallite size (nm)	Band gap (eV)	VB edge potential (eV)	CB edge potential (eV)
CeO_2	7.13 nm	2.5	2.03	-0.47
C_3N_5	8.55 nm	1.9	1.09	-0.81

Table S2. Elemental composition of C_3N_5, CeO_2 and C_3N_5/CeO_2 Composites

Catalyst	Elemental Composition (SEM EDAX) (%)				Elemental Composition (XPS) (%)			
CeO_2	Ce		O		Ce		O	
	69.7		30.3		81.4		19.6	
C_3N_5	C		N		C		N	
	29.1		70.9		39.4		60.6	
CeO_2 /C_3N_5	Ce	O	C	N	Ce	O	C	N
	2.6	29.6	27.4	40.4	2.1	20.6	35.6	41.7

Table S3. Activity comparison of some representative photocatalysts for photocatalytic hydrogen production.

SI No	Catalyst	Scavenger	Co-Catalyst	Light Source	Hydrogen evolution rate (μmol/g/h)	Reference
1	S-doped C_3N_5	TEOA	-	UV	486	S[1]
2	Cr/N-STO	Methanol	Pt	UV	106.7	**S[2]**
3	NiO/C_3N_5	TEOA	-	UV	357	S[3]
4	CdS/C_3N_5	TEOA	-	UV	502.11	S[4]
5	$C_3N_4/CeCO_3OH/CeO_2$	TEOA	-	UV	764	S[5]
6	CeO_2/MoS_2	Na_2SO_3/Na_2S	-	UV	112.5	S[6]
7	CeO_2/MXene	TEOA	-	UV	454.32	S[7]
8	$Rh–TiO_2–CeO_2$	Methanol	-	UV	48.3	S[8]
9	NR-CeO_2/CdS	Lactic Acid	-	Visible	444	S[9]
10	CeO_2/C_3N_5	Methanol	-	Visible	1256	**This Work**

References

1. Guan, X.; Fawaz, M.; Sarkar, R.; Lin, C.-H.; Li, Z.; Lei, Z.; Nithinraj, P. D.; Kumar, P.; Zhang, X.; Yang, J.-H. J. J. o. M. C. A., S-doped C 3 N 5 derived from thiadiazole for efficient photocatalytic hydrogen evolution. *Journal of Materials Chemistry A* **2023,** *11* (24), 12837-12845.
2. Yu, H.; Ouyang, S.; Yan, S.; Li, Z.; Yu, T.; Zou, Z. J. J. o. M. C., Sol–gel hydrothermal synthesis of visible-light-driven Cr-doped SrTiO 3 for efficient hydrogen production. *Journal of Materials Chemistry* **2011,** *21* (30), 11347-11351.
3. LIU, M.-y.; WANG, J.-y.; Lian, D.; Xian, L.; ZHANG, L. J. J. o. F. C.; Technology, Nickel oxide modified C3N5 photocatalyst for enhanced hydrogen evolution performance. *Journal of Fuel Chemistry* **2022,** *50* (2), 243-249.
4. Wang, B.; Qiao, H.; Guan, P.; Yang, B.; Liu, B. J. C. I., Fabrication of CdS/C3N5 photocatalyst for enhanced H2 production. *Composite Interfaces* **2023,** *30* (2), 147-161.
5. Tong, R.; Sun, Z.; Zhong, X.; Wang, X.; Xu, J.; Yang, Y.; Xu, B.; Wang, S.; Pan, H. J. C., Enhancement of visible-light photocatalytic hydrogen production by CeCO3OH in g-C3N4/CeO2 system. *ChemCatChem* **2019,** *11* (3), 1069-1075.
6. Yadav, A. A.; Hunge, Y. M.; Kang, S.-W. J. C., Visible light-responsive CeO2/MoS2 composite for photocatalytic hydrogen production. *Catalysts* **2022,** *12* (10), 1185.
7. Zhu, H.; Fu, X.; Zhou, Z. J. A. o., 3D/2D heterojunction of CeO2/ultrathin MXene nanosheets for photocatalytic hydrogen production. *omega* **2022,** *7* (25), 21684-21693.
8. Hong, J.-W. J. C., Development of visible-light-driven Rh–TiO2–CeO2 hybrid photocatalysts for hydrogen production. *Catalysts* **2021,** *11* (7), 848.
9. Liu, Z.; Zhuang, Y.; Dong, L.; Mu, H.; Li, D.; Zhang, F.; Xu, H.; Xie, H. J. A. A. E. M., Enhancement mechanism of photocatalytic hydrogen production activity of CeO2/CdS by morphology regulation. *Applied Energy Materials* **2023,** *6* (14), 7722-7736.